

# Every Little Helps: Building Knowledge Graph Foundation Model with Fine-grained Transferable Multi-modal Tokens

Yichi Zhang<sup>1</sup> Zhuo Chen<sup>1</sup> Lingbing Guo<sup>1</sup> Wen Zhang<sup>1</sup> Huajun Chen<sup>1</sup>

## Abstract

**Multi-modal knowledge graph reasoning** (MMKGR) aims to predict the missing links by exploiting both graph structure information and multi-modal entity contents. Most existing works are designed for a transductive setting, which learns dataset-specific embeddings and struggles to generalize to new KGs. Recent knowledge graph foundation models (KGFM) improve cross-KG transfer, but they mainly exploit structural patterns and ignore rich multi-modal signals. We address these gaps by proposing a token-based foundation model (TOFU) for MMKGR, which exhibits strong generalization across different MMKGs. TOFU discretizes structural, visual, and textual information into modality-specific tokens. TOFU then employs a hierarchical fusion architecture with mixture-of-message mechanisms, aiming to process these tokens and obtain transferable features for MMKGR. Experimental results on 17 transductive, inductive, and fully-inductive MMKGs show that TOFU consistently outperforms strong KGFM and MMKGR baselines, delivering strong performance on unseen MMKGs.

## 1. Introduction

Multi-modal knowledge graph reasoning (MMKGR) (Chen et al., 2024) aims to discover new relational links among multi-modal entities. Unlike traditional KGR, MMKGR must model complex relational patterns (Bordes et al., 2013) while effectively integrating heterogeneous modality information (e.g., images and texts), which makes model design challenging and has attracted increasing research attention.

Most MMKGR methods (Guo et al., 2025b; Zhang et al., 2025b; Jian et al., 2025) are developed under a transductive

<sup>1</sup>Zhejiang University, Zhejiang, China. Correspondence to: Yichi Zhang <zhangyichi.each@zju.edu.cn>, Zhuo Chen <chen.zhuo@zju.edu.cn>, Lingbing Guo <lbguo@zju.edu.cn>, Wen Zhang <zhang.wen@zju.edu.cn>, Huajun Chen <huajun-sir@zju.edu.cn>.

Paradigm Comparison of MMKGR/KGFM and TOFU

|       | Multi-modality | Entity-wise Embedding Table | Cross-KG Generalization | Model Granularity  |
|-------|----------------|-----------------------------|-------------------------|--------------------|
| MMKGR | Yes            | Yes                         | No                      | Entity             |
| KGFM  | No             | No                          | Yes                     | Subgraph Structure |
| TOFU  | Yes            | No                          | Yes                     | Token              |

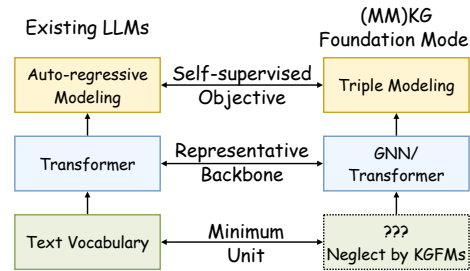


Figure 1. A comparison between MMKGR/KGFM and TOFU, along with insights gained from current large language models.

setting: they train and evaluate on the same MMKG with fixed entity and relation sets, and rely on dataset-specific entity/relation embeddings. These models perform well on the training KG but generalize poorly to unseen entities, unseen relations, or new KGs, which limits their reusability. Recently, more works are considering the KG foundation model (KGFM) (Galkin et al., 2024; Cui et al., 2024), which is inspired by the paradigm of large foundation models (Touvron et al., 2023) that have strong generalization capability. However, these KGFM mainly extract transferable structural patterns, largely ignoring richer multi-modal signals, even if existing research (Xie et al., 2017) indicates that multi-modal contents significantly aid reasoning outcomes. This leads to a natural question: *Can we build KGFM by considering multi-source information from both structure and multi-modal contents?*

To achieve this goal, two key challenges arise: (C1) How to define transferable features across different modalities? (C2) How to design effective architectures that fully exploit these transferable features? As illustrated in Figure 2, existing MMKGR studies rarely consider cross-KG transferability of multi-modal information, while various KGFM approaches focus on exploring structural features. Current

MMKGR work primarily relies on shallow embeddings, whereas KGFM mainly leverages graph neural networks (GNNs) (Zhu et al., 2021) to learn structural features, lacking exploration on transferable multi-modal fusion.

We draw inspiration from the design of successful foundation models, such as LLMs. LLMs convert raw text into a fixed vocabulary, using subword-level tokens to convert text into tokens as the minimum units and basics of the foundation model, and employ representative neural network backbones such as transformers (Vaswani et al., 2017) and MoE (Dai et al., 2024). Finally, a self-supervised training objective is defined for large-scale pre-training. For language, the specific objective is the auto-regressive profile for texts. The key idea is that a stable tokenization scheme plus a unified backbone yields a reusable model that can be applied across diverse tasks and domains. The vocabulary serves as a self-contained module providing foundational text processing capabilities. We posit that a similar token-based design principle can also benefit MMKGR.

Therefore, we propose a **TO**ken-based MMKG **Fo**Undation model (TOFU). TOFU builds a KGFM with fine-grained transferable multi-modal tokens by treating all modalities, including structural, visual, and textual information, as discrete token sequences. For visual and textual information, TOFU borrows tokenizers and pre-trained codebooks from the vision/text foundation models (Devlin et al., 2019) to process the modality information into token-level embedding sequences. For the structural modality, TOFU encodes entities into discrete tokens based on their relative positions in sampled context subgraphs. TOFU further employs a hierarchical fusion architecture that consists of a structural encoder and a multi-modal encoder to obtain the transferable modality features, which are fused with a relation-aware adaptive gate. Through this module, we obtain transferable entity and relation representations. TOFU further proposes a global aggregation module that propagates compositional multi-modal messages via a mixture-of-messages mechanism to perform multi-modal triple modeling on context subgraphs. Importantly, TOFU removes entity-/relation-specific embedding tables and instead learns to utilize transferable multi-modal features, enabling a single model to be pre-trained and fine-tuned across different MMKGs with a unified objective, and to support both zero-shot and supervised fine-tuning transfer. To verify the effectiveness of TOFU, we conduct comprehensive experiments on 17 MMKGs with transductive, inductive, and fully-inductive settings. Through experimentation, we demonstrate that TOFU exhibits robust zero-shot capabilities after pretraining, which further improve upon fine-tuning and surpass baseline performance. We also provide in-depth analyses and visualizations to explain the behavior of key components and to justify our design choices. Our contribution can be summarized as:

- **Token-based Paradigm.** Motivated by current LLMs, we first propose a token-based paradigm to build a foundation model for MMKGR. This paradigm processes different modalities into discrete token representations through specific methods and models them unifiedly.
- **Foundation Architecture.** We introduce TOFU, a token-based foundation architecture for MMKGR that combines a hierarchical fusion module and a global propagation module to capture transferable multi-modal features from both local and global views. TOFU can complete pre-training and fine-tuning with a unified objective, and possesses the ability to induce new entities and relations across different MMKGs.
- **Extensive Experiments.** We conduct comprehensive experiments on 17 MMKGs with transductive, inductive, and fully-inductive settings for performance evaluation. Further explorations are made to show the rationality and interpretability of TOFU.

## 2. Related Works

**MMKG Reasoning.** MMKG Reasoning (MMKGR) (Chen et al., 2024) aims to predict the missing triples in the given MMKG. Existing MMKGR works (Jian et al., 2025; Gao et al., 2025; Guo et al., 2025b) mainly focus on transductive settings, which learns separate multi-modal embeddings for different entities. Although these studies have designed various elegant multi-modal fusion methods (Zhang et al., 2025a;b; Guo et al., 2025a), few have addressed how to leverage the transferability of modal information to build more generalizable foundational models (Yang et al., 2025) for achieving transferable multi-modal reasoning.

**Foundation Model for KG.** Traditional KG completion and reasoning models (Bordes et al., 2013; Sun et al., 2019; Ivana et al., 2019) learn separate embeddings for entities and relations in the static KG, which can not be generalized to new entities and relations. Knowledge graph foundation model (KGFM) (Cui et al., 2024) aims to build a foundation model for KG reasoning, which possesses cross-KG transfer capabilities, enabling generalization to new knowledge graphs with unseen entities and relations during training. ULTRA (Galkin et al., 2024) proposes relative relation representations as transferable features to build a foundation model. MOTIF (Huang et al., 2025) further extends ULTRA to a relational hyper-graph to learn the relation patterns for generalization. KG-ICL (Cui et al., 2024) modeling the generalizable features with in-context graph prompts. These methods focus on structural information as transferable features, which neglect the importance of multi-modal information in the KG. Some MMKG models like IndMKG (Yang et al., 2025) have explored transfer learning of multi-modal information, but have not pursued further research

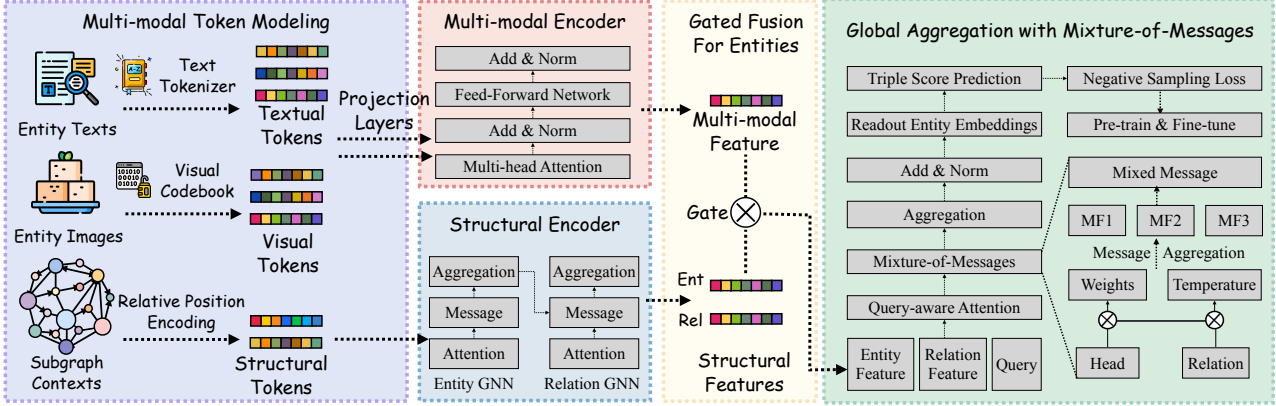


Figure 2. An overview of our TOFU framework. TOFU first models each modality (structure/visual/textual) into discrete tokens and employs a hierarchical fusion architecture to obtain the transferable entity and relation features, which consists of a structural encoder, a multi-modal encoder, and a fusion gate. Finally, TOFU applies global aggregation with a mixture-of-message mechanism to obtain multi-source information from the MMKG to make the MMKGR prediction based on the query-informed entity representations.

along the KGF pathway. In this work, we will explore KGF that considers both structural patterns in the KG and multi-modal content of entities to build the first multi-modal KGF with a fine-grained token-based modeling approach.

### 3. Preliminaries

**MMKG Reasoning (MMKGR).** MMKGs can be represented as  $\mathcal{KG} = (\mathcal{E}, \mathcal{R}, \mathcal{T}, \mathcal{M})$  where  $\mathcal{E}, \mathcal{R}$  are the entity and relation set.  $\mathcal{T} = \{(h, r, t) | h, t \in \mathcal{E}, r \in \mathcal{R}\}$  consists of structured triple represent factual knowledge.  $\mathcal{M} = (\mathcal{M}_{vis}, \mathcal{M}_{txt})$  represents the multi-modality content set of the KG. In this paper, we mainly focus on two common modalities: visual (vis) and textual (txt). Given a query  $(h, r, ?)$ , MMKGR aims to predict the missing entity in the query by taking into account both the structural information in  $\mathcal{T}$  and the multimodal content in  $\mathcal{M}$ . In practice, the inverse relation  $r^{-1}$  and inverse triple  $(t, r^{-1}, h)$  for every relation  $r$  and triple  $(h, r, t)$  would be added into the KG. If the head entity  $h$  and relation  $r$  appearing in a query have already been seen during training, we refer to it as **transductive** MMKGR; otherwise, it is referred to as **inductive** MMKGR. In the transductive setting, the model can perform MMKGR by learning separate embeddings for entities and relations. In the inductive setting, however, new entities and/or relations may appear only at inference time, which requires more appropriate designs to enable knowledge transfer to these unseen entities and relations.

**KG Foundation Model.** KGF aims to achieve transferable KGR by modeling the transferable features in the KGs. A KGF can be trained on several KGs  $\mathcal{D}_{train} = \{\mathcal{KG}_{train}^{(i)}\}_{i=1}^m$  and evaluate on other KGs  $\mathcal{D}_{test} = \{\mathcal{KG}_{test}^{(i)}\}_{i=1}^n$ , which correspond to the original KG's train/valid/test splits, so the training and testing data may share the same entity/relation sets (transductive) or may not

(inductive). This places higher demands on KGF's generalization capabilities. In this paper, all KGs considered are MMKGs with additional multi-modal information.

## 4. Methodology

In this section, we present the details of the TOFU framework. We first describe how TOFU captures fine-grained transferable features from MMKGs and then encodes them into local- and global-aware multi-modal knowledge representations for MMKGR.

### 4.1. Transferable Multi-modal Tokens

Compared with traditional KGR methods, the key advantage of KGFs lies in their ability to capture transferable features and patterns that can be generalized across different KGs. In TOFU, we propose a token-based transferable modeling approach, where different modalities are uniformly represented as discrete tokens.

#### 4.1.1. VISUAL AND TEXTUAL TOKENS

The multi-modal contents (visual and textual information) of entities can be easily processed into discrete tokens. Given an entity  $e$ , its multi-modal contents  $\mathcal{M}_{vis}(e), \mathcal{M}_{txt}(e)$  can be processed into a token sequence as:

$$\mathcal{X}_m(e) = \mathcal{Q}_m(\mathcal{M}_m(e)) = [x_{m,1}, x_{m,2}, \dots, x_{m,n_m}] \quad (1)$$

where  $\mathcal{Q}_m$  is the processor for modality  $m \in \{txt, vis\}$ , transferring entity modality content into  $n_m$  discrete tokens.  $\mathcal{Q}_m$  is a text tokenizer or a pre-trained VQ-VAE network (van den Oord et al., 2017) for visual modality.  $x_{m,i}$  are the corresponding vectors of the semantic ids in the codebook of  $\mathcal{Q}_m$ . Compared to existing MMKGR methods, this token-based approach provides finer-grained multimodal features for subsequent modeling. Since these features are derived

from a fixed pre-trained codebook, they exhibit strong generalization ability across different entities.

#### 4.1.2. STRUCTURAL TOKEN MODELING

In contrast to visual and textual contents, the structural modality cannot be directly extracted from an entity in isolation. Traditional KGR methods usually define entity-wise learnable embeddings to model structural information, which is simple but lacks transferability to unseen entities. Following existing KGFM, TOFU employs relative position tokens to capture entity structures within a subgraph. Given a triple  $(h, r, t)$ , a subgraph  $\mathcal{KG}' = (\mathcal{E}', \mathcal{R}', \mathcal{T}')$  is randomly sampled from the original  $\mathcal{KG}$  with the  $k$ -hop neighbors of  $(h, r, t)$ . For every  $e \in \mathcal{E}'$ , we compute its shortest-path distances to the head and tail entities, forming a positional tuple  $[d(e, h), d(e, t)]$ , where  $d(\cdot)$  is the distance function. This tuple, which represents the entity's relative structural role, is then mapped to a corresponding learnable embedding. These embeddings effectively form a discrete codebook of structural tokens, analogous to the visual and textual tokens.

### 4.2. Hierarchical Local Fusion

Next, we propose a hierarchical architecture to achieve multi-level multi-modal fusion and local feature aggregation for entities. A key distinction is that while our visual and textual tokens are derived from pre-trained models, the structural tokens are initialized without pre-trained weights. Therefore, we first develop a structural encoder (SE) to learn contextualized structural representations for entities and relations within their local subgraph contexts.

#### 4.2.1. STRUCTURAL ENCODER

The structural encoder is tasked with capturing transferable structural patterns from the subgraph context. As previously described, structural information is represented by a learnable codebook of position embeddings. Therefore, we employ an  $L_1$ -layer graph neural network (GNN) as the subgraph structural encoder (SE). Given a query  $q = (h, r, ?)$  and its subgraph context  $\mathcal{KG}'$ , we assign the entity and relation hidden representations in the  $i$ -th layer of the SE as  $\mathcal{H}_{ent}^{(i)}, \mathcal{H}_{rel}^{(i)}$ . Here,  $\mathcal{H}_{ent}^{(0)}$  is the structural token embeddings and  $\mathcal{H}_{rel}^{(0)}$  is initialized by zero vectors. A learnable query vector shared by all relations is added to the query relation  $r$ . In each layer, the entity and relation representations are iteratively updated as:

$$\mathcal{H}_{ent}^{(i+1)} = \mathbf{AGG}_{n \in \mathcal{N}(e)}(\mathbf{MSG}(\mathcal{H}_{ent}^{(i)}, \mathcal{H}_{rel}^{(i)}, n, q)) \quad (2)$$

$$\mathcal{H}_{rel}^{(i+1)} = \mathbf{AGG}_{n \in \mathcal{N}(r)}(\mathbf{MSG}(\mathcal{H}_{ent}^{(i)}, \mathcal{H}_{rel}^{(i)}, n, q)) \quad (3)$$

Here,  $\mathcal{N}(e), \mathcal{N}(r)$  represent the neighbors of the entities and relations in  $\mathcal{KG}'$ .  $\mathbf{AGG}, \mathbf{MSG}$  are the aggregation

and message functions in the GNN, respectively. We concatenate the query  $q$  and hidden representations and project it with one MLP as the message, which would be further aggregated with attention-based aggregation and a pooling layer. Finally, we can obtain the structural entity and relation representations in the subgraph contexts from SE, which can be denoted as  $\mathcal{H}_{ent}^{(L_1)}, \mathcal{H}_{rel}^{(L_1)}$ . These features consist of structural representations based on relative positions and would be further used in the subsequent modules. More design details of SE are presented in Appendix A.1.

#### 4.2.2. MULTI-MODAL ENCODER AND GATED FUSION

We further employ a multi-modal encoder (ME) to encode the multi-modal contents for entities. We employ a transformer encoder (Vaswani et al., 2017) with multi-head attention (MHA) and feed-forward network (FFN) modules to capture the multi-modal feature of entities as:

$$f_{mm}(e) = \mathbf{Transformer}([\mathbf{ENT}], \mathcal{X}_{mm}(e)) \quad (4)$$

$$\mathcal{X}_{mm}(e) = [\mathcal{P}_{txt}(\mathcal{X}_{txt}(e)), \mathcal{P}_{vis}(\mathcal{X}_{vis}(e))] \quad (5)$$

where  $[\mathbf{ENT}]$  is a learnable readout token shared by all entities. We first project the visual and textual tokens with projection layers  $\mathcal{P}_{txt}$  and  $\mathcal{P}_{vis}$  to align their dimensions with the transformer input, and then take the output representation of  $[\mathbf{ENT}]$  as the multi-modal representation of entity  $e$ . In summary, we can obtain two feature vectors  $f_{str}(e), f_{mm}(e)$  for entity  $e$ , which represent its structural features in the subgraph contexts and multi-modal features from its raw contents. These two features are fused into a unified representation for subsequent prediction. We employ a gated-fusion (GF) module to achieve adaptive fusion as:

$$f_{all}(e) = g_{str} \odot f_{str}(e) + g_{mm} \odot f_{mm}(e) \quad (6)$$

$$g_{str}, g_{mm} = \sigma(\mathcal{P}_{all}([f_{str}(e), f_{mm}(e)])) \quad (7)$$

Here we employ another projection layer  $\mathcal{P}_{all}$  and sigmoid function  $\sigma$  to project the concatenated structural and multi-modal features into adaptive gate weights.

### 4.3. Global Propagation with Mixture-of-Messages

In the above process, we achieve transferable entity and relation modeling with fine-grained tokens from three modalities. We further design the global propagation (GP) module to propagate the multi-modal representations to candidate entities for final prediction. GP is a  $L_2$ -layers GNN that also updates the entity representations iteratively as:

$$\widehat{\mathcal{H}}_{ent}^{(j+1)} = \mathbf{AGG}_{n \in \mathcal{N}(r)}(\mathbf{MSG}(\widehat{\mathcal{H}}_{ent}^{(j)}, \widehat{\mathcal{H}}_{rel}^{(j)}, n, q)) \quad (8)$$

For a given query  $q = (h, r, ?)$ , the new entity representation matrix  $\widehat{\mathcal{H}}_{ent}^{(0)}$  is initialized with  $f_{all}$  for the query entity, and others are assigned as zero vectors.  $\widehat{\mathcal{H}}_{rel}^{(0)}$  is initialized with

the output of SE. Moreover, **MSG** and **AGG** are another group of message and aggregation functions. In TOFU, we propose a mixture-of-messages (MiM) module as **MSG**. MiM first employs a query-aware attention module as:

$$\alpha_{(h,r,t)} = \sigma(\mathcal{P}_2 \delta(\mathcal{P}_1([\widehat{\mathcal{H}}_{ent}(h), \widehat{\mathcal{H}}_{rel}(r), \widehat{\mathcal{H}}_{ent}(t)]))) \quad (9)$$

Here,  $\mathcal{P}_1, \mathcal{P}_2$  are two projection layers and  $\delta, \sigma$  are the ReLU (Glorot et al., 2011) and sigmoid activation functions respectively. For a triple  $(h, r, t)$ , their hidden representations are concatenated as the input for attention weights. The message function of MiM is designed as:

$$m_{h \rightarrow t} = \sum_{i=1}^k \beta_i m_{h \rightarrow t, i} \quad \beta_i = \frac{\exp(\gamma_i / \tau_i)}{\sum_{j=1}^k \exp(\gamma_j / \tau_j)} \quad (10)$$

$$\gamma_i = \mathcal{P}_3([\widehat{\mathcal{H}}_{ent}(h), \widehat{\mathcal{H}}_{rel}(r)]) \quad \tau_i = \mathcal{P}_4(\widehat{\mathcal{H}}_{rel}(r)) \quad (11)$$

Here, we employ a series of heterogeneous message functions  $m_{h \rightarrow t, i}$  combined by weight  $\beta_i$ , which is defined by  $\gamma_i$  and  $\tau_i$ .  $\gamma_i$  is the gate logits estimated with a projection layer and  $\tau_i$  is the relation-aware temperature. With such a design, the weights for  $m_{h \rightarrow t, i}$  can be dynamically adjusted by the head and relation (query) contexts. This is because we found that different message functions excel at handling different relations. Therefore, we designed MiM to dynamically combine various message functions, enabling them to adapt to different relational information and enhance their generalization capabilities across diverse KGs. In practice, the different message functions can be denoted as:

$$m_{h \rightarrow t, i} = \widehat{\mathcal{H}}_{ent}(h) \otimes_i \widehat{\mathcal{H}}_{rel}(r) \quad (12)$$

Here,  $\otimes_i$  is the operator for the  $i$ -th message function. We employ three classic KGR model TransE (Bordes et al., 2013), Distmult (Yang et al., 2015), and RotatE (Sun et al., 2019) as  $\otimes_i$ , which are addition, element-wise product, and complex rotation, respectively. After message passing, TOFU further aggregates the messages with a sum operation. A score layer  $\mathcal{P}_{score}$  is defined to calculate the score of a candidate entity  $t$  for the query  $(h, r, ?)$  as:

$$\mathcal{S}(h, r, t) = \mathcal{P}_{score}(\widehat{\mathcal{H}}_{ent}^{(L_2)}(t)) \quad (13)$$

Note that the query encoded with multi-modal information has been propagated to all entities. Therefore, the final hidden representations of the query message can be directly used for KGR. The training objective can be denoted as:

$$\mathcal{L}_{kgr} = - \sum_{(h, r, t) \in \mathcal{T}} \log \frac{\exp(\mathcal{S}(h, r, t))}{\sum_{t' \in \mathcal{E}} \exp(\mathcal{S}(h, r, t'))} \quad (14)$$

Following traditional KGR settings, all entities except the ground-truth one are treated as negative labels. Throughout the entire design, we do not define any entity-specific or

Table 1. The KGFM experiment results on 17 MMKGs.

| Method          | Transductive |        | Inductive |        | Fully-Inductive |        | Overall |        |       |
|-----------------|--------------|--------|-----------|--------|-----------------|--------|---------|--------|-------|
|                 | MRR          | Hit@10 | MRR       | Hit@10 | MRR             | Hit@10 | MRR     | Hit@10 |       |
| Supervised SOTA | 42.79        | 55.12  | 48.40     | 65.13  | 16.55           | 29.63  | 37.61   | 50.89  |       |
| ULTRA           | zero-shot    | 34.34  | 49.64     | 49.63  | 67.70           | 39.45  | 60.73   | 38.24  | 55.43 |
|                 | fine-tune    | 44.32  | 57.13     | 50.80  | 68.57           | 39.03  | 60.35   | 44.22  | 59.90 |
| KG-ICL          | zero-shot    | 42.73  | 53.66     | 53.77  | 71.43           | 41.05  | 63.55   | 44.28  | 59.13 |
|                 | fine-tune    | 42.95  | 54.41     | 54.33  | 72.60           | 44.38  | 66.48   | 45.30  | 60.46 |
| MOTIF           | zero-shot    | 35.34  | 51.47     | 49.93  | 69.50           | 38.73  | 60.70   | 38.71  | 56.82 |
|                 | fine-tune    | 44.42  | 57.43     | 52.80  | 70.77           | 37.93  | 58.98   | 44.37  | 60.15 |
| TOFU            | zero-shot    | 44.65  | 56.87     | 53.51  | 71.72           | 43.44  | 66.15   | 45.93  | 61.67 |
|                 | fine-tune    | 46.87  | 59.13     | 54.77  | 72.45           | 43.22  | 65.68   | 47.41  | 63.02 |

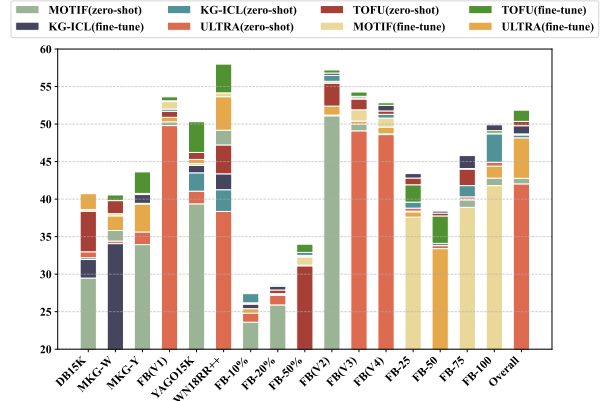


Figure 3. Detailed MRR results on the MMKGs. We annotate three baselines and the TOFU’s performance across zero-shot and fine-tuning settings for each dataset, sorted in ascending order.

relation-specific parameters. Instead, we build an MMKGR model with cross-KG generalization capabilities from the ground up using fine-grained multi-modal tokens. TOFU can be pre-trained on existing MMKGs to enable zero-shot inference on new MMKGs, or fine-tuned using the training data of new MMKGs. The training objective remains identical in both the pre-training and fine-tuning phases.

## 5. Experiments

### 5.1. Experiment Settings

**Datasets.** The KGs used in traditional KGFM experiments lack multi-modal information. We collected and retained 17 MMKG of them, which can be divided into three categories: transductive datasets, inductive datasets, and fully-inductive datasets. More about the 17 MMKGs are presented in B.2.

**Baselines and Metrics.** For transductive experiments, we employ 21 recent SOTA MMKG methods. Their detailed information is presented in Appendix B.2. For KGFM experiments, we compare our method with ULTRA, MOTIF, IndMKG, and KG-ICL with both pre-training and fine-tuning settings. We employed multiple distinct settings in the KGFM experiments, including transductive, inductive, and fully-inductive MMKGR experiments. Following

Table 2. Single-dataset transductive experiment results on three standard MMKGR benchmarks.

| Model       | DB15K        |              |              |              | MKG-W        |              |              |              | MKG-Y        |              |              |              | Overall      |              |              |              |
|-------------|--------------|--------------|--------------|--------------|--------------|--------------|--------------|--------------|--------------|--------------|--------------|--------------|--------------|--------------|--------------|--------------|
|             | MRR          | Hit@1        | Hit@3        | Hit@10       |
| IKRL        | 26.82        | 14.09        | 34.93        | 49.09        | 32.36        | 26.11        | 34.75        | 44.07        | 33.22        | 30.37        | 34.28        | 38.26        | 30.80        | 23.52        | 34.65        | 43.81        |
| TBKGC       | 28.40        | 15.61        | 37.03        | 49.86        | 31.48        | 25.31        | 33.98        | 43.24        | 33.99        | 30.47        | 35.27        | 40.07        | 31.29        | 23.80        | 35.43        | 44.39        |
| TransAE     | 28.09        | 21.25        | 31.17        | 41.17        | 30.00        | 21.23        | 34.91        | 44.72        | 28.10        | 25.31        | 29.10        | 33.03        | 28.73        | 22.60        | 31.73        | 39.64        |
| MMKRL       | 26.81        | 13.85        | 35.07        | 49.39        | 30.10        | 22.16        | 34.09        | 44.69        | 36.81        | 31.66        | 39.79        | 45.31        | 31.24        | 22.56        | 36.32        | 46.46        |
| RSME        | 29.76        | 24.15        | 32.12        | 40.29        | 29.23        | 23.36        | 31.97        | 40.43        | 34.44        | 31.78        | 36.07        | 39.09        | 31.14        | 26.43        | 33.39        | 39.94        |
| VBKGC       | 30.61        | 19.75        | 37.18        | 49.44        | 30.61        | 24.91        | 33.01        | 40.88        | 37.04        | 33.76        | 38.75        | 42.30        | 32.75        | 26.14        | 36.31        | 44.21        |
| OTKGE       | 23.86        | 18.45        | 25.89        | 34.23        | 34.36        | 28.85        | 36.25        | 44.88        | 35.51        | 31.97        | 37.18        | 41.38        | 31.24        | 26.42        | 33.11        | 40.16        |
| MANS        | 28.82        | 16.87        | 36.58        | 49.26        | 30.88        | 24.89        | 33.63        | 41.78        | 29.03        | 25.25        | 31.35        | 34.49        | 29.58        | 22.34        | 33.85        | 41.84        |
| MMRNS       | 32.68        | 23.01        | 37.86        | 51.01        | 35.03        | 28.59        | 37.49        | 47.47        | 35.93        | 30.53        | 39.07        | 45.47        | 34.55        | 27.38        | 38.14        | 47.98        |
| IMF         | 32.25        | 24.20        | 36.00        | 48.19        | 34.50        | 28.77        | 36.62        | 45.44        | 35.79        | 32.95        | 37.14        | 40.63        | 34.18        | 28.64        | 36.59        | 44.75        |
| QEB         | 28.18        | 14.82        | 36.67        | 51.55        | 32.38        | 25.47        | 35.06        | 45.32        | 34.37        | 29.49        | 36.95        | 42.32        | 31.64        | 23.26        | 36.23        | 46.40        |
| VISTA       | 30.42        | 22.49        | 33.56        | 45.94        | 32.91        | 26.12        | 35.38        | 45.61        | 30.45        | 24.87        | 32.39        | 41.53        | 31.26        | 24.49        | 33.78        | 44.36        |
| NATIVE      | 34.30        | 25.08        | 39.48        | 51.35        | 36.84        | 29.94        | 40.06        | 49.39        | 39.21        | 35.03        | 41.21        | 46.25        | 36.78        | 30.02        | 40.25        | 49.00        |
| AdaMF       | 32.51        | 21.31        | 39.67        | 51.68        | 34.27        | 27.21        | 37.86        | 47.21        | 38.06        | 33.49        | 40.44        | 45.48        | 34.95        | 27.34        | 39.32        | 48.12        |
| SNAG        | 36.30        | 27.40        | 41.10        | 53.00        | 37.30        | 30.20        | 40.50        | 50.30        | 39.10        | 34.70        | 41.08        | 46.70        | 37.57        | 30.77        | 40.89        | 50.00        |
| MyGO        | 37.72        | 30.08        | 41.26        | 52.21        | 36.10        | 29.78        | 38.54        | 47.75        | 38.44        | 35.01        | 39.84        | 44.19        | 37.42        | 31.62        | 39.88        | 48.05        |
| MoMok       | 39.57        | <b>32.38</b> | <b>43.45</b> | <b>54.14</b> | 35.89        | 30.38        | 37.54        | 46.13        | 37.91        | 35.09        | 39.20        | 43.20        | 37.79        | 32.62        | 40.06        | 47.82        |
| K-ON        | 38.10        | 30.13        | 42.77        | 53.59        | 36.64        | 30.05        | 38.72        | 48.26        | 35.83        | 32.56        | 37.34        | 42.45        | 36.86        | 30.91        | 39.61        | 48.10        |
| MCKGC       | <b>39.79</b> | <b>31.92</b> | <b>43.80</b> | <b>54.66</b> | 36.88        | <b>31.32</b> | 38.92        | 47.43        | 38.92        | <b>35.49</b> | 40.57        | 45.21        | 38.53        | <b>32.91</b> | 41.10        | 49.10        |
| APKGC       | 36.40        | 28.20        | 41.30        | 52.70        | 37.40        | 30.60        | 40.40        | 50.10        | 38.41        | 34.52        | 40.27        | 45.02        | 37.40        | 31.11        | 40.66        | 49.27        |
| LMBKGC      | 37.23        | 27.78        | 42.75        | 54.71        | 38.46        | 31.20        | 41.78        | <b>51.46</b> | 40.03        | 33.89        | <b>43.11</b> | <b>50.81</b> | 38.57        | 30.96        | <b>42.55</b> | <b>52.33</b> |
| <b>TOFU</b> | 39.01        | 31.80        | 42.34        | 53.14        | <b>40.40</b> | <b>34.39</b> | <b>42.98</b> | <b>51.66</b> | <b>43.72</b> | <b>40.50</b> | <b>45.25</b> | <b>49.77</b> | <b>41.04</b> | <b>35.56</b> | <b>43.52</b> | <b>51.52</b> |

the classic KGC evaluation protocol, we report the Mean Reciprocal Rank (MRR) and Hit@K (K=1,3,10) results as evaluation metrics under filter setting (Bordes et al., 2013).

**Implementation Details.** For transductive experiments, we train and evaluate on the same MMKG. For other experiments, we pre-train TOFU on DB15K, MKG-W, MKG-Y, and FB15K-237(v1) and evaluate on 17 MMKGs as zero-shot performance. Besides, we fine-tune the pre-trained model on these MMKGs to obtain the fine-tune performance. This setting is consistent with the previous KGFM. All experiments are conducted on NVIDIA A100 GPUs. Detailed hyper-parameter settings are presented in Appendix B.3.

## 5.2. Main Experiments

In the main experiments, we investigate the performance of TOFU as a KGFM from two complementary perspectives:

**(1). Pre-training and Fine-tuning on 17 MMKGs.** We first compare TOFU with several recent KGFM baselines under two settings: (i) zero-shot reasoning after pre-training, and (ii) supervised reasoning after task-specific fine-tuning. As summarized in Table 1 and Figure 3, we report results for both settings across three standard scenarios: transductive, inductive, and fully-inductive. More fine-grained, dataset-wise results are provided in Table 4.

From these results, we observe that TOFU (i) achieves consistently strong performance under the transductive setting, showing its ability to capture rich structural patterns within a fixed graph; (ii) generalizes robustly in inductive and fully-inductive settings, attaining performance comparable to KG-ICL and approaching supervised SOTA results on several datasets; (iii) already surpasses several fine-tuned

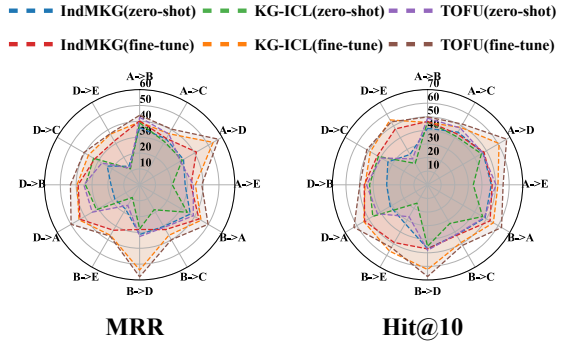


Figure 4. Single-MMKG transfer experiments. A→B denotes training on dataset A and testing on dataset B. The abbreviation for MMKG is as follows: YAGO15K(A), MKG-Y(B), MKG-W(C), WN18RR++(D), FB15K-237(E). We compare TOFU with two baselines under both zero-shot and fine-tuning settings.

baselines in the zero-shot setting, especially on MMKGs with informative visual and textual modalities, demonstrating effective exploitation of multi-modal cues for cross-KG transfer; and (iv) maintains a balanced performance across 17 MMKGs and three evaluation settings, indicating its advantage as a general-purpose KG foundation model rather than a model tailored to a specific scenario.

**(2). Comparison with IndMKG.** The above experiments mainly validate the effectiveness of TOFU in the standard KGFM setting. We now turn to a more challenging evaluation that explicitly stresses *transferability* across different MMKGs, and compare TOFU with transferable MMKGR methods such as IndMKG (Yang et al., 2025). Following the protocol in the IndMKG paper, we conduct single-source transfer experiments between pairs of MMKGs, i.e., we pre-train on dataset A and directly perform KGR on dataset

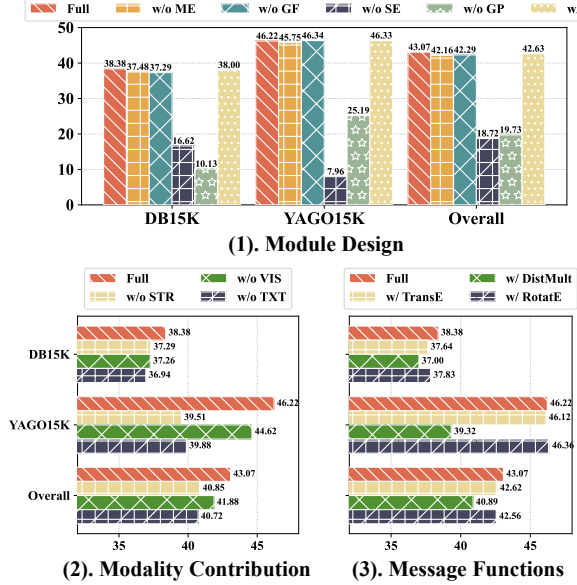


Figure 5. Ablation study on module design, modality contribution, and message function selections. The ablation study is conducted on 5 MMKGs separately, including DB15K, MKG-W, MKG-Y, YAGO15K, and WN18RR++. Overall results represent the average of them. We report the MRR results in the figures.

B without any additional training on B ( $A \rightarrow B$ ). Due to the lack of fully functional released code, we keep their experimental configurations unchanged and directly reuse the experimental settings and reported results from IndMKG to ensure a fair and comparable evaluation.

Under this setting, TOFU achieves state-of-the-art performance, consistently outperforming IndMKG and KG-ICL in both zero-shot and fine-tuning scenarios (Figure 4). The gains are particularly pronounced in the zero-shot regime, where the model must rely purely on its pre-trained multi-modal and structural priors to adapt to a new graph. This highlights that TOFU is not merely competitive on in-domain benchmarks, but also exhibits strong cross-dataset and cross-graph transfer, which is crucial for practical deployment on diverse real-world KGs.

### 5.3. Transductive MMKGR Experiments

The main experiments primarily evaluate cross-graph transferability. To further assess the effectiveness of TOFU under the standard MMKGR setting, we additionally conduct transductive experiments where training and evaluation are performed on the same MMKG.

We present the results on three benchmarks in Table 2. The results indicate that TOFU consistently outperforms traditional MMKGR methods in terms of overall performance, with especially notable gains on MKG-W and MKG-Y while maintaining a sub-optimal leading position on DB15K.

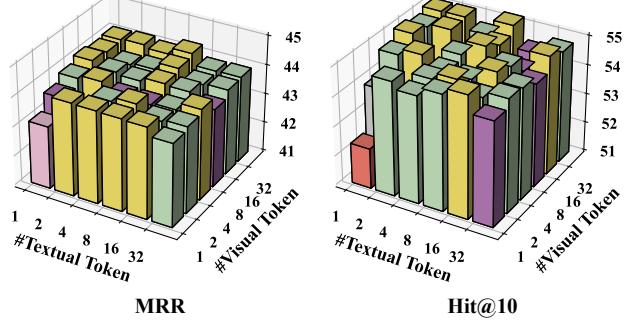


Figure 6. The influence of text/visual token number.

On average, TOFU achieves the best results across all metrics. A more fine-grained inspection reveals that TOFU shows larger improvements on Hit@1, while being slightly weaker on Hit@10 compared to some baselines. Since all baselines adopt separate entity embeddings, whereas TOFU discards this design and relies purely on token-level multi-modal modeling, this suggests a trade-off: the lack of dedicated entity embeddings may moderately affect coarse-grained ranking, but does not hinder—and may even benefit—precise ranking. In summary, the transductive MMKGR experiments show that token-level modeling of all modal information yields positive gains for the MMKGR task.

### 5.4. Ablation Study and Further Exploration

We further conduct an ablation study to validate the reasonability of our design. The ablation study consists of three aspects: the overall module design, the modality contribution, and the message function selection.

As presented in Figure 5(1), each key module in TOFU positively contributes to the final performance. Although components such as GF do not yield consistent gains on every single dataset, their averaged effect over the 5 MMKGs is clearly beneficial. The results also indicate that SE and GP, the two GNN modules, still bring the largest improvements, underscoring that structural patterns and subgraph contexts are still significant in MMKGR, and multi-modal information plays complementary roles. Importantly, these multi-modal representations are foundational for TOFU: without them, structure-aware modules such as GP would lack informative node and relation features to exploit.

Figure 5(2) further examines the contribution of each modality by removing one modality at a time. All three modalities are useful, with textual information generally providing the strongest signal, while the relative importance of visual and textual cues varies across MMKGs. It is worth noting that w/o SE and w/o structural tokens represent two distinct experimental settings, yet both collectively confirm that structural information in the subgraph contexts is still the dominant modality for MMKGR tasks.

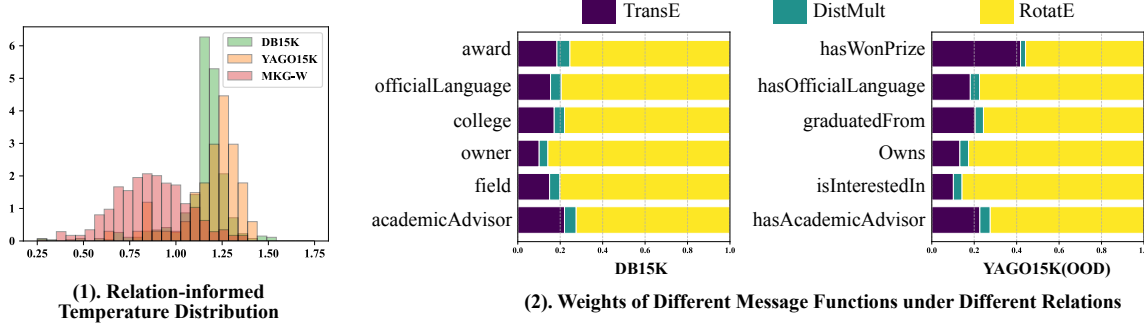


Figure 7. Case study on the mixture-of-message modules. We visualize the distribution of temperature  $\gamma_i$  for different relations and the weights for the three message functions under different query relations. Note that YAGO15K is an OOD dataset in this experiment.

Next, we conducted further investigations into the message function within the GP module, exploring three classic functions: TransE, DistMult, and RotatE. We observe that the MiM module, which aggregates these heterogeneous messages via a MoE mechanism, achieves the best overall performance across datasets. Although a single message function may occasionally outperform MiM on a specific MMKG, MiM offers more stable and robust gains when averaged over multiple graphs, suggesting that different relation patterns are better captured by different message types.

Finally, we study the effect of the number of visual and textual tokens  $N_{vis}, N_{txt}$  in Figure 6. A fundamental principle is that model performance tends to increase gradually as the token count grows. However, considering the balance between efficiency and performance, we typically opt for a relatively small value such as 8 or 16. Note that the structural modality is represented by a single token whose features are directly aggregated by SE, leading to a much higher information density per structural token than for visual or textual tokens. We also provide parameter efficiency analysis of TOFU in Appendix B.5.

### 5.5. Case Study and Visualized Analysis

To provide a more intuitive understanding of our design, we conduct a case study focusing on the GP module in TOFU. For the proposed mixture-of-messages mechanism, we visualize two key components: (i) the distribution of relation-guided temperature values, and (ii) the weights assigned to the three base message functions.

First, we visualized the temperature distribution in Figure 7(1). Following the KGFM configuration outlined earlier, we conducted pre-training on the DB15K/MKG-W/MKG-Y and FB15K-237(v1) datasets. For this temperature distribution visualization, we selected two in-distribution datasets and one out-of-distribution (OOD) dataset, YAGO15K. We visualized the mean logits before the sigmoid obtained for different relations across these datasets. The distributions differ noticeably across datasets, indicating that the relation-guided temperature adapts to the

relation patterns of each graph. Moreover, the temperature distribution on the OOD YAGO15K dataset is clearly distinct from those on the pre-training datasets, yet still leads to performance gains, suggesting that this mechanism can generalize to unseen relational configurations.

We also visualized the weights of the three message functions in MiM. Several patterns emerge: first, the three weights for different relations show distinct differences, yet all exhibit relatively low dependence on distmult. The variations primarily concentrate on the TransE and RotatE message functions. Second, message weight distributions for similar relations across different datasets exhibit certain similarities. For example, the *academicAdvisor* relation in DB15K and the *hasAcademicAdvisor* relation in YAGO15K have very similar weight distributions. This emerges even though relation texts are not used during pre-training, indicating that TOFU captures transferable relation patterns and reuses them on OOD datasets. In other words, the message mixture learned during pre-training exhibits strong relational generalization on new MMKGs, which is crucial for robust MMKGR under distribution shifts.

## 6. Conclusion

In this paper, we focus on building a foundation model for MMKGR. We propose a new token-based framework TOFU to model the multi-modality (structure/visual/text) in MMKGs as discrete tokens. We first propose the token modeling process for three modalities and further propose a hierarchical architecture to accomplish MMKGR with the multi-modal fine-grained tokens with mixture-of-messages. Extensive experiments on 17 MMKGs under transductive, inductive, and fully-inductive settings demonstrate that TOFU consistently outperforms existing KGFM and MMKGR baselines. In-depth explorations are made to further show the rationality and mechanism interpretability of TOFU. In the future, the integration of more MMKG tasks like entity linking and entity alignment towards a unified multi-modal KGFM would be further explored.

## Impact Statement

This paper explores the topic of foundation models for MMKGR. Throughout this research, all libraries and datasets utilized were sourced from open-source communities and platforms. We strictly adhered to scientific ethics during the research process, refraining from any unethical data collection or experimentation. We hope the proposed method can serve societal endeavors, such as KG completion and reasoning across various fields including healthcare and industrial production.

## References

Bordes, A., Usunier, N., García-Durán, A., Weston, J., and Yakhnenko, O. Translating Embeddings for Modeling Multi-relational Data. In *NIPS*, pp. 2787–2795, 2013.

Cao, Z., Xu, Q., Yang, Z., He, Y., Cao, X., and Huang, Q. OTKGE: Multi-modal Knowledge Graph Embeddings via Optimal Transport. In *NeurIPS*, 2022.

Chen, Z., Zhang, Y., Fang, Y., Geng, Y., Guo, L., Chen, X., Li, Q., Zhang, W., Chen, J., Zhu, Y., Li, J., Liu, X., Pan, J. Z., Zhang, N., and Chen, H. Knowledge graphs meet multi-modal learning: A comprehensive survey. *CoRR*, abs/2402.05391, 2024.

Chen, Z., Fang, Y., Zhang, Y., Guo, L., Chen, J., Pan, J. Z., Chen, H., and Zhang, W. Noise-powered multi-modal knowledge graph representation framework. In *COLING*, pp. 141–155. Association for Computational Linguistics, 2025.

Cui, Y., Sun, Z., and Hu, W. A Prompt-Based Knowledge Graph Foundation Model for Universal In-Context Reasoning. In *NeurIPS*, 2024.

Dai, D., Deng, C., Zhao, C., Xu, R. X., Gao, H., Chen, D., Li, J., Zeng, W., Yu, X., Wu, Y., Xie, Z., Li, Y. K., Huang, P., Luo, F., Ruan, C., Sui, Z., and Liang, W. Deepseekmoe: Towards ultimate expert specialization in mixture-of-experts language models. In *ACL (1)*, pp. 1280–1297. Association for Computational Linguistics, 2024.

Devlin, J., Chang, M., Lee, K., and Toutanova, K. BERT: pre-training of deep bidirectional transformers for language understanding. In *NAACL-HLT (1)*, pp. 4171–4186. Association for Computational Linguistics, 2019.

Fey, M. and Lenssen, J. E. Fast graph representation learning with pytorch geometric. *CoRR*, abs/1903.02428, 2019.

Galkin, M., Yuan, X., Mostafa, H., Tang, J., and Zhu, Z. Towards foundation models for knowledge graph reasoning. In *ICLR*. OpenReview.net, 2024.

Gao, Y., Zhang, F., Zhang, Z., Min, X., and Zhuang, F. Mixed-curvature multi-modal knowledge graph completion. In *AAAI*, pp. 11699–11707. AAAI Press, 2025.

Glorot, X., Bordes, A., and Bengio, Y. Deep sparse rectifier neural networks. In *AISTATS*, volume 15 of *JMLR Proceedings*, pp. 315–323. JMLR.org, 2011.

Guo, L., Zhang, Y., Bo, Z., Chen, Z., Sun, M., Zhang, Z., Zhang, W., and Chen, H. K-ON: stacking knowledge on the head layer of large language model. In *AAAI*, pp. 11745–11753. AAAI Press, 2025a.

Guo, Y., Ma, Q., Li, H., Ning, Q., Zhan, F., Gu, Y., Yu, G., and Guo, S. Lbmkgc: Large model-driven balanced multi-modal knowledge graph completion. In *The Thirty-ninth Annual Conference on Neural Information Processing Systems*, 2025b.

Huang, X., Barceló, P., Bronstein, M. M., Ceylan, İ. İ., Galkin, M., Reutter, J. L., and Orth, M. A. R. How expressive are knowledge graph foundation models? In *ICML*. OpenReview.net, 2025.

Ivana, B., Carl, A., and Timothy, M. H. Tucker: Tensor factorization for knowledge graph completion. In *EMNLP/IJCNLP (1)*, pp. 5184–5193. Association for Computational Linguistics, 2019.

Jian, Y., Luo, X., Li, Z., Zhang, M., Zhang, Y., Xiao, K., and Hou, X. APKGC: noise-enhanced multi-modal knowledge graph completion with attention penalty. In *AAAI*, pp. 15005–15013. AAAI Press, 2025.

Kingma, D. P. and Ba, J. Adam: A method for stochastic optimization. In *ICLR (Poster)*, 2015.

Lee, J., Chung, C., Lee, H., Jo, S., and Whang, J. J. VISTA: Visual-Textual Knowledge Graph Representation Learning. In *EMNLP (Findings)*, pp. 7314–7328. Association for Computational Linguistics, 2023a.

Lee, J., Chung, C., and Whang, J. J. Ingram: Inductive knowledge graph embedding via relation graphs. In *ICML*, volume 202 of *Proceedings of Machine Learning Research*, pp. 18796–18809. PMLR, 2023b.

Li, X., Zhao, X., Xu, J., Zhang, Y., and Xing, C. IMF: Interactive Multimodal Fusion Model for Link Prediction. In *WWW*, pp. 2572–2580. ACM, 2023.

Liu, Y., Li, H., García-Durán, A., Niepert, M., Oñoro-Rubio, D., and Rosenblum, D. S. MMKG: multi-modal knowledge graphs. In *ESWC*, volume 11503 of *Lecture Notes in Computer Science*, pp. 459–474. Springer, 2019.

Lu, X., Wang, L., Jiang, Z., He, S., and Liu, S. MMKRL: A robust embedding approach for multi-modal knowledge

graph representation learning. *Appl. Intell.*, 52(7):7480–7497, 2022.

Lv, X., Han, X., Hou, L., Li, J., Liu, Z., Zhang, W., Zhang, Y., Kong, H., and Wu, S. Dynamic anticipation and completion for multi-hop reasoning over sparse knowledge graph. In *EMNLP (1)*, pp. 5694–5703. Association for Computational Linguistics, 2020.

Paszke, A., Gross, S., Massa, F., Lerer, A., Bradbury, J., Chanan, G., Killeen, T., Lin, Z., Gimelshein, N., Antiga, L., Desmaison, A., Kopf, A., Yang, E. Z., DeVito, Z., Raison, M., Tejani, A., Chilamkurthy, S., Steiner, B., Fang, L., Bai, J., and Chintala, S. Pytorch: An imperative style, high-performance deep learning library. In *NeurIPS*, pp. 8024–8035, 2019.

Peng, Z., Dong, L., Bao, H., Ye, Q., and Wei, F. Beit v2: Masked image modeling with vector-quantized visual tokenizers. *CoRR*, abs/2208.06366, 2022.

Sergieh, H. M., Botschen, T., Gurevych, I., and Roth, S. A Multimodal Translation-Based Approach for Knowledge Graph Representation Learning. In *\*SEM@NAACL-HLT*, pp. 225–234. Association for Computational Linguistics, 2018.

Sun, Z., Deng, Z.-H., Nie, J.-Y., and Tang, J. RotatE: Knowledge Graph Embedding by Relational Rotation in Complex Space. In *ICLR (Poster)*. OpenReview.net, 2019.

Teru, K. K., Denis, E. G., and Hamilton, W. L. Inductive relation prediction by subgraph reasoning. In *ICML*, volume 119 of *Proceedings of Machine Learning Research*, pp. 9448–9457. PMLR, 2020.

Touvron, H., Lavril, T., Izacard, G., Martinet, X., Lachaux, M., Lacroix, T., Rozière, B., Goyal, N., Hambro, E., Azhar, F., Rodriguez, A., Joulin, A., Grave, E., and Lampe, G. Llama: Open and efficient foundation language models. *CoRR*, abs/2302.13971, 2023.

van den Oord, A., Vinyals, O., and Kavukcuoglu, K. Neural discrete representation learning. In *NIPS*, pp. 6306–6315, 2017.

Vaswani, A., Shazeer, N., Parmar, N., Uszkoreit, J., Jones, L., Gomez, A. N., Kaiser, L., and Polosukhin, I. Attention is all you need. In *NIPS*, pp. 5998–6008, 2017.

Wang, M., Wang, S., Yang, H., Zhang, Z., Chen, X., and Qi, G. Is Visual Context Really Helpful for Knowledge Graph? A Representation Learning Perspective. In *ACM Multimedia*, pp. 2735–2743. ACM, 2021.

Wang, X., Meng, B., Chen, H., Meng, Y., Lv, K., and Zhu, W. TIVA-KG: A multimodal knowledge graph with text, image, video and audio. In *ACM Multimedia*, pp. 2391–2399. ACM, 2023.

Wang, Z., Li, L., Li, Q., and Zeng, D. Multimodal Data Enhanced Representation Learning for Knowledge Graphs. In *IJCNN*, pp. 1–8. IEEE, 2019.

Xie, R., Liu, Z., Luan, H., and Sun, M. Image-embodied Knowledge Representation Learning. In *IJCAI*, pp. 3140–3146. ijcai.org, 2017.

Xu, D., Xu, T., Wu, S., Zhou, J., and Chen, E. Relation-enhanced Negative Sampling for Multimodal Knowledge Graph Completion. In *ACM Multimedia*, pp. 3857–3866. ACM, 2022.

Yang, B., Yih, W.-t., He, X., Gao, J., and Deng, L. Embedding Entities and Relations for Learning and Inference in Knowledge Bases. In *ICLR (Poster)*, 2015.

Yang, J., Jiang, X., Gao, Y., Yang, L. T., and Yang, J. Generalize to fully unseen graphs: Learn transferable hyper-relation structures for inductive link prediction. In *ACM Multimedia*, pp. 1274–1282. ACM, 2024a.

Yang, J., Yang, S., Gao, Y., Yang, J., and Yang, L. T. Multimodal contextual interactions of entities: A modality circular fusion approach for link prediction. In *ACM Multimedia*, pp. 8374–8382. ACM, 2024b.

Yang, S., Yang, J., Jiang, X., Gao, Y., Yang, L. T., Luo, R., and Yang, J. Towards Multimodal Inductive Learning: Adaptively Embedding MMKG via Prototypes. In *WWW*, pp. 109–118. ACM, 2025.

Zhang, Y. and Zhang, W. Knowledge graph completion with pre-trained multimodal transformer and twins negative sampling. *CoRR*, abs/2209.07084, 2022.

Zhang, Y., Chen, M., and Zhang, W. Modality-aware negative sampling for multi-modal knowledge graph embedding. In *IJCNN*, pp. 1–8. IEEE, 2023.

Zhang, Y., Chen, Z., Guo, L., Xu, Y., Hu, B., Liu, Z., Zhang, W., and Chen, H. Native: Multi-modal knowledge graph completion in the wild. In *SIGIR*, pp. 91–101. ACM, 2024a.

Zhang, Y., Chen, Z., Liang, L., Chen, H., and Zhang, W. Unleashing the power of imbalanced modality information for multi-modal knowledge graph completion. In *LREC/COLING*, pp. 17120–17130. ELRA and ICCL, 2024b.

Zhang, Y., Chen, Z., Guo, L., Xu, Y., Hu, B., Liu, Z., Zhang, W., and Chen, H. Multiple heads are better than one: Mixture of modality knowledge experts for entity representation learning. In *ICLR*. OpenReview.net, 2025a.

Zhang, Y., Chen, Z., Guo, L., Xu, Y., Hu, B., Liu, Z., Zhang, W., and Chen, H. Tokenization, fusion, and augmentation:

Towards fine-grained multi-modal entity representation.  
In *AAAI*, pp. 13322–13330. AAAI Press, 2025b.

Zhu, Z., Zhang, Z., Xhonneux, L. A. C., and Tang, J. Neural bellman-ford networks: A general graph neural network framework for link prediction. In *NeurIPS*, pp. 29476–29490, 2021.

Table 3. Statistical information of the 17 MMKG datasets used in the experiments.

| Dataset                      | Train   |           |         | Valid   |           |         | Test    |           |         |
|------------------------------|---------|-----------|---------|---------|-----------|---------|---------|-----------|---------|
|                              | #Entity | #Relation | #Triple | #Entity | #Relation | #Triple | #Entity | #Relation | #Triple |
| <b>Transductive MMKGs</b>    |         |           |         |         |           |         |         |           |         |
| <b>DB15K</b>                 | 12842   | 279       | 79222   | 12842   | 279       | 9902    | 12842   | 279       | 9904    |
| <b>MKG-W</b>                 | 15000   | 169       | 34196   | 15000   | 169       | 4276    | 15000   | 169       | 4274    |
| <b>MKG-Y</b>                 | 15000   | 28        | 21310   | 15000   | 28        | 2665    | 15000   | 28        | 2663    |
| <b>YAGO15K</b>               | 15283   | 32        | 86020   | 15283   | 32        | 12289   | 15283   | 32        | 24577   |
| <b>WN9</b>                   | 6555    | 9         | 11741   | 6555    | 9         | 1337    | 6555    | 9         | 1319    |
| <b>WN18RR++</b>              | 41105   | 11        | 86835   | 41105   | 11        | 3034    | 41105   | 11        | 3134    |
| <b>FB15K-237-10%</b>         | 11512   | 237       | 27211   | 11512   | 237       | 15624   | 11512   | 237       | 18150   |
| <b>FB15K-237-20%</b>         | 13166   | 237       | 54423   | 13166   | 237       | 16963   | 13166   | 237       | 19776   |
| <b>FB15K-237-50%</b>         | 14149   | 237       | 136057  | 14149   | 237       | 17449   | 14149   | 237       | 20324   |
| <b>Inductive MMKGs</b>       |         |           |         |         |           |         |         |           |         |
| <b>FB15K-237(v1)</b>         | 1594    | 180       | 4245    | 1594    | 180       | 489     | 1093    | 180       | 411     |
| <b>FB15K-237(v2)</b>         | 3668    | 215       | 9799    | 3668    | 215       | 1166    | 2501    | 215       | 947     |
| <b>FB15K-237(v3)</b>         | 3668    | 215       | 17986   | 3668    | 215       | 2194    | 2504    | 215       | 1731    |
| <b>FB15K-237(v4)</b>         | 4707    | 219       | 27203   | 4707    | 219       | 3352    | 3051    | 219       | 2840    |
| <b>Fully-Inductive MMKGs</b> |         |           |         |         |           |         |         |           |         |
| <b>FB-25</b>                 | 5190    | 163       | 91571   | 4097    | 216       | 5716    | 4097    | 216       | 5716    |
| <b>FB-50</b>                 | 5190    | 153       | 85375   | 4445    | 205       | 3879    | 4445    | 205       | 3879    |
| <b>FB-75</b>                 | 4659    | 134       | 62809   | 2792    | 186       | 3106    | 2792    | 186       | 3106    |
| <b>FB-100</b>                | 4659    | 134       | 62809   | 2624    | 77        | 2329    | 2624    | 77        | 2329    |

## A. Method Design

### A.1. Details of the Structural Encoder

As mentioned in Section 4.2.1, we employ a GNN as a structural encoder to capture the structural information from the subgraph contexts with relative position embeddings. This design refers to KG-ICL (Cui et al., 2024). We first randomly sample the subgraph contexts of a given triple  $(h, r, t)$  and transfer it into structural tokens. Then, based on the aforementioned message passing approach, alternately learn the transferable features of relations and entities, which serve as the output of the SE module. The entity representation learning process can be denoted as:

$$\mathbf{h}^{(i+1)} = \delta \left( \text{MaxPooling}_{t \in \mathcal{N}(h)} \left( \text{message}(\mathbf{h}^{(i)}, \mathbf{r}^{(i)}, \mathbf{t}^{(i)}, q) \right) \right) \quad (15)$$

$$\text{message}(\mathbf{h}^{(i)}, \mathbf{r}^{(i)}, \mathbf{t}^{(i)}, q) = \alpha_{r,q} \mathcal{P}_{ent}^{(i)} \left( [\mathbf{h}^{(i)}, \mathbf{r}^{(i)}, q] \right) \quad \alpha_{r,q} = \sigma \left( \mathcal{P}_{attn}^{(i)} \left( [\mathbf{r}^{(i)}, q] \right) \right) \quad (16)$$

Here, we employ a max-pooling layer with ReLU activation  $\delta$  to aggregate the message information. The message is based on the central node  $h$ , edge  $r$ , and the query  $q$ .  $\alpha_{r,q}$  is the adaptive attention weights and  $\mathcal{P}_{ent}^{(i)}, \mathcal{P}_{attn}^{(i)}$  are projection layers. We denote a certain entity in the full hidden representation matrix  $\mathcal{H}_{ent}^{(i)}$  as  $\mathbf{h}^{(i)}$ . The relation aggregation also employs a similar design, aggregating messages around the relation with max-pooling and query-aware attention. Through this design, we constructed a GNN module as a Self-Encoder to extract structured representations of a query  $q = (h, r, ?)$  based on structural tokens encoded from relative positions. These representations will be further utilized in subsequent design stages.

## B. Experiments

### B.1. Dataset Information

As presented in Table 3, our MMKG datasets used in this paper can be divided into three categories:

- **Transductive MMKG Datasets:** DB15K (Liu et al., 2019), MKG-W (Xu et al., 2022), MKG-Y (Xu et al., 2022), YAGO15K (Liu et al., 2019), WN9 (Xie et al., 2017), WN18RR++ (Xu et al., 2022), FB15K-237-10%/20%/50% (Lv et al., 2020). These datasets have fixed entity and relation sets during training and evaluation.

Table 4. The full results of the KGFM experiments on 17 MMKG datasets.

| Dataset         | Metrics              | Supervised SOTA | ULTRA     |           | KG-ICL    |           | MOTIF     |           | TOFU      |           |       |
|-----------------|----------------------|-----------------|-----------|-----------|-----------|-----------|-----------|-----------|-----------|-----------|-------|
|                 |                      |                 | pre-train | fine-tune | pre-train | fine-tune | pre-train | fine-tune | pre-train | fine-tune |       |
| Transductive    | <b>DB15K</b>         | <b>MRR</b>      | 37.23     | 32.98     | 40.72     | 32.19     | 31.95     | 29.48     | 38.59     | 38.38     | 38.62 |
|                 |                      | <b>Hit@10</b>   | 54.71     | 48.36     | 56.59     | 45.11     | 45.23     | 46.34     | 55.76     | 52.73     | 53.02 |
|                 | <b>MKG-W</b>         | <b>MRR</b>      | 38.46     | 34.41     | 37.77     | 34.10     | 34.07     | 35.82     | 38.07     | 39.80     | 40.55 |
|                 |                      | <b>Hit@10</b>   | 51.46     | 45.68     | 49.13     | 39.23     | 43.37     | 46.99     | 49.60     | 50.71     | 51.70 |
|                 | <b>MKG-Y</b>         | <b>MRR</b>      | 40.03     | 35.62     | 39.35     | 40.76     | 40.61     | 33.94     | 39.44     | 43.72     | 43.65 |
|                 |                      | <b>Hit@10</b>   | 50.81     | 42.09     | 45.86     | 46.94     | 47.03     | 44.04     | 46.00     | 49.77     | 50.06 |
|                 | <b>YAGO15K</b>       | <b>MRR</b>      | 43.03     | 41.06     | 45.29     | 43.50     | 44.48     | 39.37     | 44.74     | 46.22     | 50.31 |
|                 |                      | <b>Hit@10</b>   | 54.49     | 54.20     | 58.16     | 53.43     | 54.69     | 54.21     | 58.14     | 59.99     | 62.89 |
|                 | <b>WN9</b>           | <b>MRR</b>      | 92.30     | 26.72     | 90.23     | 94.68     | 95.15     | 34.56     | 91.20     | 94.31     | 95.15 |
|                 |                      | <b>Hit@10</b>   | 94.70     | 50.26     | 91.96     | 95.15     | 95.15     | 63.84     | 92.57     | 95.00     | 95.15 |
| Inductive       | <b>WN18RR++</b>      | <b>MRR</b>      | 55.26     | 38.36     | 53.65     | 41.25     | 43.37     | 49.18     | 54.16     | 47.22     | 57.99 |
|                 |                      | <b>Hit@10</b>   | 67.55     | 54.17     | 64.15     | 48.28     | 51.53     | 58.64     | 64.26     | 56.03     | 67.87 |
|                 | <b>FB15K-237-10%</b> | <b>MRR</b>      | 21.90     | 24.80     | 25.40     | 27.40     | 26.00     | 23.60     | 25.40     | 26.10     | 26.18 |
|                 |                      | <b>Hit@10</b>   | 33.70     | 39.80     | 41.10     | 43.30     | 41.60     | 38.40     | 41.10     | 41.52     | 41.70 |
|                 | <b>FB15K-237-20%</b> | <b>MRR</b>      | 24.70     | 27.20     | 27.40     | 28.50     | 28.40     | 25.90     | 27.30     | 27.89     | 28.65 |
|                 |                      | <b>Hit@10</b>   | 39.10     | 43.60     | 44.50     | 45.40     | 45.60     | 42.20     | 44.40     | 44.45     | 45.95 |
|                 | <b>FB15K-237-50%</b> | <b>MRR</b>      | 29.30     | 32.40     | 32.50     | 32.90     | 32.40     | 31.20     | 32.30     | 31.11     | 33.99 |
|                 |                      | <b>Hit@10</b>   | 45.80     | 52.60     | 52.80     | 52.00     | 49.90     | 50.80     | 52.30     | 50.43     | 52.97 |
|                 | <b>FB15K-237(V1)</b> | <b>MRR</b>      | 45.70     | 49.80     | 50.90     | 52.00     | 53.10     | 50.30     | 53.00     | 51.71     | 53.63 |
|                 |                      | <b>Hit@10</b>   | 58.90     | 65.60     | 67.00     | 67.80     | 70.00     | 69.20     | 70.20     | 68.05     | 70.00 |
| Fully-Inductive | <b>FB15K237(V2)</b>  | <b>MRR</b>      | 51.00     | 51.20     | 52.40     | 56.50     | 56.80     | 51.10     | 55.70     | 55.45     | 57.21 |
|                 |                      | <b>Hit@10</b>   | 67.20     | 70.00     | 71.00     | 74.90     | 76.80     | 71.60     | 74.40     | 74.69     | 76.05 |
|                 | <b>FB15K-237(V3)</b> | <b>MRR</b>      | 47.60     | 49.10     | 50.40     | 53.50     | 53.70     | 50.00     | 51.90     | 53.34     | 54.27 |
|                 |                      | <b>Hit@10</b>   | 63.70     | 65.40     | 66.30     | 69.50     | 70.40     | 69.20     | 68.40     | 69.71     | 70.12 |
|                 | <b>FB15K-237(V4)</b> | <b>MRR</b>      | 46.60     | 48.60     | 49.60     | 51.30     | 52.50     | 48.70     | 50.80     | 51.75     | 52.84 |
|                 |                      | <b>Hit@10</b>   | 64.50     | 67.70     | 68.40     | 69.90     | 70.60     | 67.70     | 69.50     | 70.75     | 71.17 |
|                 | <b>FB-25</b>         | <b>MRR</b>      | 22.30     | 38.80     | 38.30     | 39.60     | 43.40     | 38.40     | 37.60     | 42.81     | 41.91 |
|                 |                      | <b>Hit@10</b>   | 37.10     | 64.00     | 63.50     | 65.60     | 69.40     | 64.00     | 62.10     | 69.51     | 69.00 |
|                 | <b>FB-50</b>         | <b>MRR</b>      | 18.90     | 33.80     | 33.40     | 34.10     | 38.40     | 33.80     | 33.40     | 38.14     | 37.76 |
|                 |                      | <b>Hit@10</b>   | 32.50     | 54.30     | 53.80     | 55.90     | 59.80     | 54.60     | 53.20     | 60.36     | 59.90 |
| Fully-Inductive | <b>FB-75</b>         | <b>MRR</b>      | 11.70     | 40.30     | 40.00     | 41.80     | 45.80     | 39.90     | 38.90     | 44.00     | 44.08 |
|                 |                      | <b>Hit@10</b>   | 21.80     | 60.40     | 59.80     | 63.30     | 66.40     | 61.40     | 59.20     | 65.12     | 64.44 |
|                 | <b>FB-100</b>        | <b>MRR</b>      | 13.30     | 44.90     | 44.40     | 48.70     | 49.90     | 42.80     | 41.80     | 48.80     | 49.12 |
|                 |                      | <b>Hit@10</b>   | 27.10     | 64.20     | 64.30     | 69.40     | 70.30     | 62.80     | 61.40     | 69.60     | 69.36 |
|                 | <b>Overall</b>       | <b>MRR</b>      | 41.68     | 42.03     | 48.17     | 48.55     | 49.78     | 42.77     | 48.69     | 50.36     | 51.85 |
|                 |                      | <b>Hit@10</b>   | 55.41     | 59.38     | 63.86     | 63.46     | 65.21     | 61.36     | 64.53     | 66.30     | 67.53 |

- Inductive MMKG Datasets:** Four inductive splits of FB15K-237(v1/v2/v3/v4) from GraIL (Teru et al., 2020). These datasets consist of new entities in the evaluation stage.
- Fully-inductive MMKG Datasets:** Four fully-inductive splits of FB15K-237(-25/-50/-75/-100) from InGram (Lee et al., 2023b), which consists of both new entities and relations in the evaluation stage, which would be more challenging for the model’s generalization capability.

The distinguishing criterion among the three types of datasets is whether their train/valid/test sets contain overlapping entities and relations. For transductive datasets, the entities and relations are consistent across the three splits. For inductive datasets, new entities are introduced in the test sets. For fully-inductive datasets, both new entities and relations would be introduced. Therefore, traditional KGR methods that learn separate embeddings for every entity and relation would not work for the inductive and fully-inductive datasets.

In the transductive experiments, we employ DB15K/MKG-W/MKG-Y as the benchmark datasets to present the transductive capability of the models. We then conduct KGFM experiments on all the mentioned datasets. We pre-train the models on DB15K/MKG-W/MKG-Y/FB15K-237-v1 and evaluate the model performance on all datasets with both zero-shot and fine-tuning settings. Given the limited availability of inductive and fully-inductive MMKG datasets at present, we can only utilize the FB15K-237 dataset, which readily provides multi-modal information. **It is important to note that we can not directly use the complete FB15K-237 dataset as pre-training data, as this would cause the model to directly leak data from the inductive and fully-inductive experiments.** Existing KGFM work has also followed this approach and employed

FB15K-237(v1) as pre-training data.

Another noteworthy point is that different MMKGs are not necessarily completely isolated. They may share some overlapping entities or triples. However, such overlap is unavoidable within KGFM, which does not mean data leakage. The corresponding multi-modal information may also exhibit minor similarities. Overall, we conduct pre-training and fine-tuning across different MMKGs to demonstrate KGFM’s ability to jointly master and apply transferable features across structural, visual, and textual domains.

## B.2. Baseline Methods

For transductive MMKGC experiments, the baselines we used for performance comparation includes IKLR (Xie et al., 2017), TBKGC (Sergieh et al., 2018), TransAE (Wang et al., 2019), MMKRL (Lu et al., 2022), RSME (Wang et al., 2021), VBGK (Zhang & Zhang, 2022), OTKGE (Cao et al., 2022), MMRNS (Xu et al., 2022), IMF (Li et al., 2023), MANS (Zhang et al., 2023), QEB (Wang et al., 2023), VISTA (Lee et al., 2023a), NATIVE (Zhang et al., 2024a), AdaMF (Zhang et al., 2024b), SNAG (Chen et al., 2025), MyGO (Zhang et al., 2025b), MoMoK (Zhang et al., 2025a), K-ON (Guo et al., 2025a), MCKGC (Gao et al., 2025), APKGC (Jian et al., 2025), LMBKGC (Guo et al., 2025b).

These baseline methods are all classic MMKGR baselines in recent years. Their common feature is that they are designed for transductive MMKGR tasks, where both training and inference are performed on the same fixed entity and relation set to make predictions for different triples. Therefore, nearly all approaches design separate entity/relation embedding tables, learning distinct structural embeddings for each entity and relation, supplemented by multi-modal information fusion to enhance the model. To achieve multimodal fusion, they designed numerous innovative architectures, including attention, transformer, MoE, diffusion, and more.

## B.3. Hyper-parameter Settings

We implement the experiments with PyTorch (Paszke et al., 2019) and PyTorch-Geometric (Fey & Lenssen, 2019). In the main experiments, we set the training epochs to 30 with a batch size of 256. The hidden dimensions of SE and GP are set to 32 for all experiments. The learning rate is set to 0.0005 using the Adam (Kingma & Ba, 2015) optimizer.

For token process, we employ BERT (Devlin et al., 2019) and BEiT (Peng et al., 2022) as text/image tokenizers respectively. BERT tokenizer is the byte pair encoding strategy to tokenize texts into subwords. BEiT employs a VQ-VAE (van den Oord et al., 2017) to process one image into  $14 \times 14$  discrete visual tokens. The embedding dimensions of the textual and visual tokens are 768 and 32, respectively. In the main experiments, we set  $N_{vis}, N_{txt}$  to 8. The GNN layers in SE and GP consist of 6 layers.

## B.4. More MMKGR Results Compared with IndMKG

We conduct more experiments with IndMKG (Yang et al., 2025), an inductive MMKGR method that follows the pre-training and fine-tuning paradigm. However, the experimental setup they employed involved transfer learning between individual MMKGs—specifically, pre-training on one MMKG and then fine-tuning on another for prediction. Strictly speaking, this approach is not entirely inductive, as the pre-trained MMKG and the fine-tuned MMKG may share overlapping entities. Nevertheless, such experiments effectively demonstrate the transfer capabilities of different models across different MMKGs.

The full experimental results are presented in Table 5. Here, we provide more inductive KGR and MMKGR baselines like InGram (Lee et al., 2023b), IMF (Li et al., 2023), MoCi (Yang et al., 2024b), ULTRA (Galkin et al., 2024), HyRel (Yang et al., 2024a), IndMKG (Yang et al., 2025), and KG-ICL (Cui et al., 2024) for comparison.

## B.5. Efficiency and Parameter Analysis of TOFU

As summarized in the main paper, TOFU differs from traditional MMKGR models in that it does not rely on separate learnable entity and relation embedding tables. For traditional MMKGR methods trained on single MMKG, it has  $O((|\mathcal{E}| + |\mathcal{R}|) \times d)$  learnable parameters where  $d$  is the embedding dimension. Instead, it is composed of a set of neural network components such as GNN layers, Transformer blocks, and projection layers, and learns a transferable model by training the parameters within these modules. It is worth noting that the token embedding tables for text and image modalities are kept fixed during training and are not updated via gradient descent. Consequently, the total number of trainable parameters in TOFU is substantially smaller than that of conventional MMKGR models that maintain large, fully

Table 5. Single MMKG transfer experiments.

| Source KG: YAGO15K  |       |       |        |         |       |        |          |       |        |           |       |        |         |       |        |     |
|---------------------|-------|-------|--------|---------|-------|--------|----------|-------|--------|-----------|-------|--------|---------|-------|--------|-----|
| Method              | MKG-Y |       |        | MKG-W   |       |        | WN18RR++ |       |        | FB15K-237 |       |        | Average |       |        |     |
|                     | MRR   | Hit@1 | Hit@10 | MRR     | Hit@1 | Hit@10 | MRR      | Hit@1 | Hit@10 | MRR       | Hit@1 | Hit@10 | MRR     | Hit@1 | Hit@10 | MRR |
| InGram              | 8.30  | 5.10  | 12.10  | 0.60    | 0.20  | 1.30   | 3.10     | 1.90  | 4.30   | 1.30      | 0.40  | 2.60   | 3.33    | 1.90  | 5.08   |     |
| IMF                 | 0.46  | 0.21  | 0.71   | 9.59    | 8.87  | 10.35  | 2.15     | 1.88  | 2.58   | 2.10      | 1.65  | 2.97   | 3.58    | 3.15  | 4.15   |     |
| MoCi                | 2.06  | 1.51  | 2.63   | 14.27   | 10.23 | 20.30  | 2.55     | 2.01  | 3.78   | 2.43      | 1.79  | 3.67   | 5.33    | 3.89  | 7.60   |     |
| ULTRA               | 35.13 | 31.13 | 42.99  | 29.91   | 23.19 | 43.10  | 27.53    | 19.19 | 42.94  | 15.96     | 9.16  | 29.83  | 27.13   | 20.67 | 39.72  |     |
| HyRel               | 10.40 | 6.30  | 13.40  | 2.30    | 0.50  | 4.10   | 4.30     | 2.10  | 8.40   | 6.10      | 2.30  | 9.30   | 5.78    | 2.80  | 8.80   |     |
| IndMKG(zero-shot)   | 36.04 | 33.00 | 41.50  | 33.38   | 27.63 | 44.72  | 31.94    | 23.68 | 47.08  | 28.70     | 19.79 | 46.89  | 32.52   | 26.03 | 45.05  |     |
| IndMKG(fine-tune)   | 39.58 | 36.20 | 45.83  | 37.15   | 31.30 | 48.80  | 53.51    | 49.90 | 60.70  | 35.14     | 27.10 | 51.80  | 41.35   | 36.13 | 51.78  |     |
| KG-ICL(zero-shot)   | 39.10 | 35.30 | 46.58  | 31.37   | 26.06 | 41.37  | 31.01    | 23.21 | 45.72  | 20.58     | 13.93 | 33.63  | 30.52   | 24.63 | 41.83  |     |
| KG-ICL(fine-tune)   | 40.26 | 36.84 | 46.60  | 33.72   | 28.63 | 43.26  | 41.34    | 37.83 | 47.99  | 32.36     | 24.77 | 47.52  | 36.92   | 32.02 | 46.34  |     |
| TOFU(zero-shot)     | 42.60 | 38.94 | 49.00  | 36.93   | 30.88 | 48.21  | 29.67    | 20.74 | 46.89  | 33.86     | 25.44 | 50.35  | 35.77   | 29.00 | 48.61  |     |
| TOFU(fine-tune)     | 43.83 | 40.50 | 49.89  | 40.48   | 34.55 | 51.50  | 57.46    | 52.74 | 67.17  | 39.19     | 30.82 | 55.56  | 45.24   | 39.65 | 56.03  |     |
| Source KG: WN18RR++ |       |       |        |         |       |        |          |       |        |           |       |        |         |       |        |     |
| Method              | MKG-W |       |        | YAGO15K |       |        | MKG-Y    |       |        | FB15K-237 |       |        | Average |       |        |     |
|                     | MRR   | Hit@1 | Hit@10 | MRR     | Hit@1 | Hit@10 | MRR      | Hit@1 | Hit@10 | MRR       | Hit@1 | Hit@10 | MRR     | Hit@1 | Hit@10 | MRR |
| InGram              | 6.50  | 2.40  | 9.60   | 5.70    | 3.70  | 9.10   | 10.30    | 8.60  | 13.50  | 7.50      | 3.50  | 11.30  | 7.50    | 4.55  | 10.88  |     |
| IMF                 | 8.75  | 8.17  | 9.41   | 6.50    | 5.22  | 8.78   | 0.50     | 0.26  | 0.81   | 2.13      | 1.66  | 3.00   | 4.47    | 3.83  | 5.50   |     |
| MoCi                | 13.56 | 10.01 | 19.85  | 9.33    | 4.78  | 17.84  | 2.14     | 1.63  | 2.66   | 2.28      | 1.65  | 3.59   | 6.83    | 4.52  | 10.99  |     |
| ULTRA               | 17.68 | 13.19 | 26.12  | 17.76   | 13.52 | 24.87  | 13.52    | 9.29  | 21.19  | 10.89     | 5.60  | 21.07  | 14.96   | 10.40 | 23.31  |     |
| HyRel               | 7.90  | 3.50  | 11.30  | 8.90    | 3.90  | 11.10  | 10.60    | 8.90  | 14.00  | 9.10      | 6.70  | 14.40  | 9.13    | 5.75  | 12.70  |     |
| IndMKG(zero-shot)   | 23.63 | 18.21 | 33.70  | 18.04   | 11.22 | 31.70  | 18.04    | 12.67 | 30.05  | 13.46     | 7.31  | 25.78  | 18.29   | 12.35 | 30.31  |     |
| IndMKG(fine-tune)   | 37.29 | 31.40 | 48.60  | 44.13   | 39.00 | 54.10  | 39.46    | 35.70 | 46.00  | 36.87     | 27.90 | 55.10  | 39.44   | 33.50 | 50.95  |     |
| KG-ICL(zero-shot)   | 33.50 | 29.33 | 41.70  | 31.38   | 21.58 | 46.51  | 34.14    | 29.85 | 42.66  | 11.62     | 8.09  | 18.17  | 27.66   | 22.21 | 37.26  |     |
| KG-ICL(fine-tune)   | 32.67 | 27.36 | 42.63  | 43.44   | 37.83 | 53.44  | 38.76    | 34.55 | 46.56  | 31.88     | 24.06 | 47.44  | 36.69   | 30.95 | 47.52  |     |
| TOFU(zero-shot)     | 27.49 | 21.82 | 39.39  | 34.50   | 30.14 | 42.55  | 35.15    | 30.19 | 44.89  | 12.13     | 7.29  | 22.06  | 27.32   | 22.36 | 37.22  |     |
| TOFU(fine-tune)     | 40.59 | 34.58 | 51.57  | 49.87   | 42.91 | 62.54  | 43.63    | 40.37 | 49.81  | 37.20     | 28.81 | 53.46  | 42.82   | 36.67 | 54.35  |     |
| Source KG: MKG-Y    |       |       |        |         |       |        |          |       |        |           |       |        |         |       |        |     |
| Method              | MKG-W |       |        | YAGO15K |       |        | WN18RR++ |       |        | FB15K-237 |       |        | Average |       |        |     |
|                     | MRR   | Hit@1 | Hit@10 | MRR     | Hit@1 | Hit@10 | MRR      | Hit@1 | Hit@10 | MRR       | Hit@1 | Hit@10 | MRR     | Hit@1 | Hit@10 | MRR |
| InGram              | 6.40  | 3.10  | 10.50  | 1.20    | 0.30  | 1.80   | 0.40     | 0.10  | 1.30   | 6.40      | 2.30  | 9.50   | 3.60    | 1.45  | 5.78   |     |
| IMF                 | 9.61  | 8.89  | 10.54  | 4.91    | 2.43  | 7.37   | 2.15     | 1.88  | 2.58   | 2.08      | 1.62  | 2.88   | 4.69    | 3.71  | 5.84   |     |
| MoCi                | 13.77 | 10.21 | 19.75  | 9.08    | 4.87  | 17.96  | 2.45     | 1.97  | 3.81   | 2.54      | 1.79  | 4.12   | 6.96    | 4.71  | 11.41  |     |
| ULTRA               | 24.46 | 17.53 | 38.51  | 34.13   | 28.75 | 43.03  | 27.01    | 17.86 | 42.15  | 11.58     | 7.19  | 20.35  | 24.30   | 17.83 | 36.01  |     |
| HyRel               | 8.70  | 4.70  | 10.90  | 6.50    | 1.40  | 8.40   | 5.10     | 1.60  | 7.70   | 10.70     | 5.10  | 13.50  | 7.75    | 3.20  | 10.13  |     |
| IndMKG(zero-shot)   | 30.33 | 23.81 | 42.54  | 36.88   | 30.70 | 48.84  | 31.33    | 22.91 | 46.95  | 17.72     | 10.75 | 32.94  | 29.07   | 22.04 | 42.82  |     |
| IndMKG(fine-tune)   | 36.79 | 30.40 | 49.10  | 44.72   | 38.60 | 55.90  | 53.73    | 49.70 | 62.30  | 36.80     | 27.10 | 56.20  | 43.01   | 36.45 | 55.88  |     |
| KG-ICL(zero-shot)   | 18.16 | 11.43 | 32.84  | 34.66   | 28.03 | 46.74  | 27.79    | 17.95 | 45.23  | 9.25      | 5.80  | 15.60  | 22.47   | 15.80 | 35.10  |     |
| KG-ICL(fine-tune)   | 32.61 | 27.29 | 42.95  | 43.19   | 37.64 | 53.10  | 28.18    | 16.59 | 47.16  | 33.09     | 25.07 | 49.01  | 34.27   | 26.65 | 48.06  |     |
| TOFU(zero-shot)     | 30.96 | 24.94 | 42.17  | 39.08   | 32.45 | 48.15  | 32.59    | 23.52 | 48.15  | 14.97     | 8.76  | 27.13  | 29.40   | 22.42 | 41.40  |     |
| TOFU(fine-tune)     | 40.00 | 33.19 | 51.42  | 49.81   | 42.71 | 62.83  | 57.99    | 53.11 | 67.47  | 37.30     | 29.21 | 53.23  | 46.28   | 39.56 | 58.74  |     |

learnable entity and relation embeddings. In addition, the number of parameters in TOFU is fixed and does not grow with the size or the number of MMKG datasets. The same set of parameters is used for training and inference across multiple datasets, which is consistent with the design philosophy of existing KGFMs. The key difference is that, on top of this foundation-model style parameter sharing, TOFU further incorporates dedicated designs for multi-modal fusion. Using the DB15K dataset as an example, the number of trainable parameters for several key components involved in our method are as follows:

- Traditional MMKGR methods: MoMoK 72.4M, MyGO 45.63M
- KGFM methods: ULTRA 0.169M, KG-ICL 0.054M, MOTIF 0.181M
- TOFU (ours): 0.248M

We observe that, compared with existing KGFM, TOFU indeed introduces a larger number of parameters. However, its parameter scale is still below 1% of that of traditional MMKGR methods. Considering that TOFU additionally incorporates multi-modal information, the extra trainable parameters introduced for multi-modal fusion remain relatively small. Overall, TOFU is parameter-efficient while achieving the benefits of multi-modality.